 CMES, vol.84, no.4, pp.333-358, 2012

A Meshless Method Using Radial Basis Functions for the Numerical Solution of Two–Dimensional Complex Ginzburg–Landau Equation

Ali Shokri[1] **and Mehdi Dehghan**[1]

Abstract: The Ginzburg–Landau equation has been used as a mathematical model for various pattern formation systems in mechanics, physics and chemistry. In this paper, we study the complex Ginzburg–Landau equation in two spatial dimensions with periodical boundary conditions. The method numerically approximates the solution by collocation method based on radial basis functions (RBFs). To improve the numerical results we use a predictor-corrector scheme. The results of numerical experiments are presented, and are compared with analytical solutions to confirm the accuracy and efficiency of the presented method.

Keywords: Two-dimensional complex Ginzburg–Landau (GL) equation, Periodic boundary conditions, Radial Basis Functions (RBFs), Multiquadrics (MQ), Thin Plate Splines (TPS), Collocation, Predictor-corrector.

1 Introduction

1.1 An introduction about Ginzburg-Landau equation

In this article, we study the following two-dimensional complex Ginzburg-Landau (GL) equation with periodical boundary condition in two dimensions,

$$u_t-(\nu+i\alpha)\,(u_{xx}+u_{yy})+(\kappa+i\beta)|u|^2u-\gamma u=0,\quad (x,y)\in\Omega,\ 0<t\leq T, \tag{1}$$

$$u(x_L,y,t)=u(x_R,y,t),\quad u(x,y_L,t)=u(x,y_R,t),\quad 0<t\leq T, \tag{2}$$

$$u_x(x_L,y,t)=u_x(x_R,y,t),\quad u_y(x,y_L,t)=u_y(x,y_R,t),\quad 0<t\leq T, \tag{3}$$

$$u(x,y,0)=u_0(x,y),\quad (x,y)\in\Omega, \tag{4}$$

[1] Department of Applied Mathematics, Faculty of Mathematics and Computer Science, Amirkabir University of Technology, No. 424, Hafez Ave., Tehran, Iran.
E-mail addresses: shokri.a@gmail.com (A. Shokri), mdehghan@aut.ac.ir; mdehghan.aut@gmail.com (M. Dehghan).

where u is a function from $\Omega \times \mathbb{R}^+$ in to $\mathbb{C}$ and Ω is a bounded domain of $\mathbb{R}^2$. The parameters $\alpha,\ \beta$ and γ are real numbers and $\nu > 0,\ \kappa > 0$. The parameter γ is the coefficient of the linear deriving term. When $\gamma \leq 0$ all solutions would decay to zero.

Originally this equation was developed by Ginzburg and Landau (Ginzburg and Landau, 1950; Wazwaz, 2009) to phenomenologically describe phase transitions in superconductors near their critical temperature and are widely used in studying the dynamics of electromagnetic behavior of a superconductor in an external magnetic field. The GL theory is also irreplaceable in investigating the dynamics of Abrikosov vortices in type II superconductors (Askerzade, 2010).

The phenomenological GL theory is one of the most elegant and powerful concepts in physics, which was applied not only to superconductivity but also to other phase transitions, to nonlinear dynamics, to dissipative systems with self-organizing pattern formation, and even to cosmology (Milošević and Geurts, 2010). It also describes the amplitude evolution of instability waves in a large variety of dissipative systems in fluid mechanics, which are close to criticality (Xu and Chang, 2011). Furthermore, it is used to model some types of chemical reactions, like the famous Belousov-Zhabotinsky reaction, to model boundary layers in multi-phase systems, to describe the development of patterns and shocks in non-equilibrium systems (Borzi, Grossauer, and Scherzer, 2005), and the theory of the origin of wind waves on a water surface (Kolesov and Rosov, 2000).

As is said in Kolesov and Rosov (2000), Equation (1) is also called the Kuramoto-Tsuzuki equation after two Japanese physicists, who, based on the physical ideas developed by Landau and Ginzburg, assumed that this equation with diffusion coefficients of the order unity and under the von Neumann boundary conditions describes the dynamics of a system of parabolic equations of the reaction-diffusion type when oscillations make its spatially homogeneous equilibrium state unstable (Kolesov and Rosov, 2000).

The existence of time-periodic solutions to the GL equations have been studied by many authors. In (Wang, 1999) Wang proved the existence of at least one time-periodic solution to the GL equations in the space dimension $n = 2$. The result was extended to the case when the space dimension is $n = 3$ in (Zhan, 2000). However, in both works the authors failed to address the uniqueness and stability of the time-periodic solution under the given boundary conditions. Zhan (Zhan, 2008) showed that the GL equations admit at least three time-periodic solutions. One of the time-periodic solutions describes the non-superconductive (or normal) state and the other one describes the superconductivity state. He also showed that the time-periodic solutions are exponentially stable.

Lega (Lega, 2001) reviewed recent works on localized solutions of the one-dimensional complex GL equation known as traveling holes. Such coherent structures seem to play an important role in the disordered dynamics displayed by GL equation at a finite distance past the Benjamin-Feir instability threshold (Lega, 2001).

Chang et al. (Chang, Ankiewicz, and Akhmediev, 2007) studied creeping solitons of the GL equation using numerical simulations and analyzed them with a low-dimensional model using the method of moments. They found the regions of existence of creeping solitons in the parameter space of this equation. Fu and Dai (H. Fu, 2010) obtained a new type of exact solitary wave solutions including chirped bright solitary-wave and chirped dark solitary-wave solutions by applying specially envelope transform and direct ansatz approach to GL equation. In (Liu, Li, and Tian, 2009) Liu and Tian presented several families of exact dark and bright soliton like solutions to the modified GL equation with variable coefficient.

Wang (Wang, 2010) proposed an efficient time-splitting Chebyshev-Tau spectral method for the Ginzburg-Landau-Schrödinger equation with zero/nonzero far-field boundary conditions. He split the Ginzburg-Landau-Schrödinger equation into linear and nonlinear parts. The nonlinear equation is solved exactly; while the linear equation is solved with Chebyshev-Tau spectral discretization in space and Crank-Nicolson method in time. In (Chen, 1997) Chen proposed a semi-implicit finite element scheme to the numerical solution of the GL model which is based on a linear finite element approximation of the order parameter and a mixed finite element discretization for the equation involving the magnetic potential.

In (Wang and Guo, 2010) Wang and Guo studied the rate of convergence of some finite difference schemes to solve the two-dimensional GL equation. Avoiding the difficulty in estimating the numerical solutions in uniform norm, they proved that all the schemes had the second-order convergence in L_2 norm by an induction argument. Xu and Chang (Xu and Chang, 2011) proposed three linearized difference schemes for solving the two dimensional GL equation with a periodic boundary condition and proved the convergence of the three schemes by an induction argument or a linearized analysis method.

1.2 An introduction about meshless methods

In the last 20 years, many researchers have shown interest in mesh-free radial basis functions (RBFs) methods. RBFs have been used for interpolation problems as well as for numerically solving partial differential equations (PDEs) (see (Brown, Ling, Kansa, and Levesley, 2005) and refs. therein).

The RBF based method is attractive not only because of its spectral accuracy when using Gaussians or multiquadrics (Brown, Ling, Kansa, and Levesley, 2005) but

it's ability to work on scattered data without using any mesh. Compared with the classical numerical method like finite element method (FEM), the meshless methods can save much time because that we have to spend much time on the mesh-generation for FEM (Duan and Tan, 2006). The price for this increased accuracy is usually ill-conditioning of the associated linear systems that need to be solved: the "uncertainty relation" shown by Schaback (Schaback, 1995a,b, 1997) is that better conditioning is associated with poorer accuracy and worse conditioning is associated with improved accuracy. Cheng et al. (Cheng, Golberg, Kansa, and Zammito, 2003) and Fedoseyev et al. (Fedoseyev, Friedman, and Kansa, 2002) demonstrated that the solutions of elliptic PDEs converge exponentially requiring orders of magnitude less discretization and operations than the traditional schemes.

The initial development of using RBFs to solving PDEs was due to the pioneering work of Kansa (Kansa, 1990a,b) who modified Hardy's multiquadric (MQ) method (Hardy, 1990) to solve partial differential equations (PDEs). Since then, solving PDEs using radial basis functions (RBFs) collocation method becomes an attractive alternative to these traditional methods because no tedious mesh generation is required.

Many positive properties of radial basis function (RBF) methods have been identified in connection with PDEs. They are grid-free numerical schemes very suitable for problems in irregular geometries. They can exploit accurate and smooth representations of the boundary, very easy to implement, and can be spectrally accurate (Platte and Driscoll, 2004). Fedoseyev et al. (Fedoseyev, Friedman, and Kansa, 2000), extended the Kansa's method to numerical solution and detection of bifurcations in 1D and 2D parameterized nonlinear elliptic PDEs. In (Demirkaya, Soh, and Ilegbusi, 2008) the pressure-velocity formulation of the Navier-Stokes equation is solved using the RBFs collocation method and the nonlinear collocated equations are solved using the Levenberg-Marquardt method. La Rocca et al. (Rocca, Rosales, and Power, 2005) proposed a meshless numerical approach for the solution of time dependent convection-diffusion problems with variable coefficients in terms of a Hermite RBF interpolation numerical scheme.

Collocation method is more successful in numerical experiments of RBF based methods than Galerkin approximation in spite of lack of theoretical analysis. Though it is very popular to use the Galerkin method in the literature of FEM, the Galerkin method is seldom used in the meshless RBFs society. One reason is that the usual Galerkin method is not so efficient as it is in FEM, because the computation of the integrals would be complicated (Zhang, 2007). For collocation method, we can not ensure that the linear system arising in this method is solvable. Actually, there are counter examples which indicate that the matrix of the linear system is singular (Hon and Schaback, 2001).

More recently Fasshauer (Fasshauer, 1996) suggested an alternative approach based on Hermite interpolation technique using RBFs, which allows not only the interpolation of a given function but also its derivatives. The convergence proof for RBF Hermite-Brikhoff interpolation was given by Wu (Wu, 1992) who also recently proved the convergence of this approach when solving PDEs (see Wu (Wu, 1998) and Schaback and Franke (Schaback and Franke, 1998)).

On the other hand, the condition number of the matrix arising in collocation method is extremely large. Accuracy and stability are other important issues to consider when employing RBFs. However, it should be pointed out that the accuracy and stability of the solution depend strongly on the type of RBF employed (Demirkaya, Soh, and Ilegbusi, 2008).

The traditional RBFs are globally defined functions which result in a full resultant coefficient matrix. To tackle this problem, a new class of compactly supported (CS) RBFs were constructed by Wendland (Wendland, 1995). In this case the resulting interpolation matrices are sparse and positive definite, which tends to improve the conditioning. Sparsity is particularly important, hence CS-RBFs are a natural choice for solving three-dimensional (3D) problems (Golberg, Chen, and Ganesh, 2000).

In most of the RBFs cases, such as multiquadrc (MQ), inverse multiquadrics (IMQ) and Gaussian (GA), the accuracy of the RBFs solution, however, depends (Dehghan and Shokri, 2009) heavily on the choice of a shape parameter c. In general, for a fixed number of centers N, smaller shape parameters produce the more accurate approximations, but also are associated with a poorly conditioned interpolation matrix. Sarra and Sturgill (Sarra and Sturgill, 2009) compared four shape parameter strategies and applied them to a battery of test problems. One strategy uses a constant shape while the other three use a different value of the shape parameter at each center. They found that the use of a constant shape parameter produces the least accurate result compare with other shape parameter strategies.

The condition number also grows (Sarra, 2005) with N for fixed values of the shape parameter c. In practice, the shape parameter must be adjusted with the number of centers in order to produce an interpolation matrix which is well conditioned enough to be inverted in finite precision arithmetic. Many researchers (e.g., (Carlson and Foley, 1991; Rippa, 1999)) have attempted to develop algorithms for selecting optimal values of the shape parameter. However, the optimal choice of the shape parameter is still an open question.

A domain decomposition procedure (or the artificial sub-sectioning method) along with a region-by-region iteration algorithm particularly tailored for parallel computation is designed in (Divo and Kassab, 2005) to address the numerical issues aris-

ing due to the nature of the coefficient matrix in radial-basis function-based meshless techniques. Overlapping domain decomposition and multilevel RBFs techniques are proposed in (Adibi and Es'haghi, 2007) for solving the two-dimensional bi-harmonic equation. In (Duan, Tang, Huang, and Lai, 2009) the project domain decomposition method is coupled with the asymmetric collocation method based on radial basis functions to solve the electrostatic problems. Authors of (Brown, Ling, Kansa, and Levesley, 2005) investigated different approximate cardinal basis function (ACBF) approaches to precondition RBFs-PDE systems. The four schemes studied in (Brown, Ling, Kansa, and Levesley, 2005) are based on solving square problems, on decay elements, solving least-square problems and both sided preconditioning. They found that the best preconditioning procedure is problem-dependent.

In (Fedoseyev, Friedman, and Kansa, 2002) Fedoseyev et al. formulated an improved Kansa's method with PDE collocation on the boundary: they added an additional set of nodes (which can lie inside or outside of the domain) adjacent to the boundary and, correspondingly, added an additional set of collocation equations obtained via collocation of the PDE on the boundary. We refer the interested reader to (Atluri and Zhu, 1998; Atluri, 2005; Atluri and Shen, 2002a,b, 2005; Dehghan and Mirzaei, 2009; Mirzaei and Dehghan, 2010; Dehghan and Ghesmati, 2010; Dehghan and Salehi, 2011; Sladek, Sladek, and Atluri, 2004; Sladek, Sladek, Hellmich, and Eberhardsteiner, 2007; Sladek, Sladek, Krivacek, and Zhang, 2003; Sladek, Sladek, Tan, and Atluri, 2008; Sladek, Sladek, and Zhang, 2004; Tatari and Dehghan, 2009; Zhu, Zhang, and Atluri, 1998) for more research works on meshless techniques.

This article is organized as follows: In Section 2, we will review using of radial basis functions to approximate the solution. An implementation of the numerical method to the problem is presented in Section 3. The numerical results are given in Section 4. In Section 5, we briefly discuss about appearance of the Ginzburg-Landau equation and one of the most important applications of this equation. We present some conclusions in Section 6. Finally some references are introduced at the end.

2 Radial basis function approximation

The following basic RBF approximation in any dimension can be defined.

Definition 2.1 *Given a function* $\phi(r),\ r \geq 0$, *and distinct centers* $\xi_1, \xi_2, \ldots, \xi_{N_c}$,

the basic RBF approximation of a distribution $u(x)$ is

$$u(x) \simeq \sum_{j=1}^{N_c} \lambda_j \phi(\|x-\xi_j\|_2) + \psi(x) \quad \text{for } x \in \Omega \subseteq \mathbb{R}^d, \tag{5}$$

where d is the dimension of the problem, and λ's are coefficients to be determined. Some well-known RBFs are listed in Table 1.

Table 1. Some well-known RBFs.

Name of function	Definition
Piecewise Smooth:	
Conical splines	$\phi(r) = r^{2k+1}$
Thin Plate (polyharmonic) Splines (TPS)	$\phi(r) = (-1)^{m+1} r^{2m} \log(r)$
Wendland functions, where p is a polynomial.	$\phi(r) = (1-r)_+^m p(r)$
Infinitely Smooth:	
Multiquadrics (MQ)	$\phi(r) = \sqrt{1+(cr)^2}$
Inverse Multiquadrics (IMQ)	$\phi(r) = \left(\sqrt{1+(cr)^2}\right)^{-1}$
Gaussian (GA)	$\phi(r) = \exp(-cr^2)$

Equation (5) can be written without the additional polynomial ψ. In that case ϕ must be *unconditionally positive definite* to guarantee the solvability of the resulting system (e.g. Gaussian or inverse multiquadrics). However, ψ is usually required when ϕ is *conditionally positive definite*, i.e., when ϕ has a polynomial growth towards infinity. Examples are thin plate splines and multiquadrics.

In our numerical method, we have used the multiquadric (MQ) RBF with constant shape parameter $c = 2$ and Thin Plate (polyharmonic) Splines (TPS) which are defined in Table 1. Since MQ is C^∞ continuous but the TPS is C^{2m-1} continuous, so higher-order thin plate splines must be used for higher-order partial differential operators. For the GL equation, $m = 3$ is used for the thin plate splines.

If $\mathscr{P}_q^d$ denotes the space of d-variate polynomials of order not exceeding q, and letting the polynomials $P_1, \ldots, P_m$ be the basis of $\mathscr{P}_q^d$ in $\mathbb{R}^d$, then the polynomial $\psi(x)$, in Equation (5), is usually written in the following form:

$$\psi(x) = \sum_{i=1}^{m} \zeta_i P_i(x), \tag{6}$$

where $m = (q-1+d)!/(d!(q-1)!)$.

To determine the coefficients $(\lambda_1, \ldots, \lambda_{N_c})$ and $(\zeta_1, \ldots, \zeta_m)$, the collocation method is used. However, in addition to the N_d equations resulting from collocating (5)

at the N_d data points, an extra m equations are required. This is insured by the following m conditions for (5),

$$\sum_{j=1}^{N_c} \lambda_j P_i(x_j) = 0, \quad i = 1, \ldots, m. \tag{7}$$

In a similar representation as (5), for any linear partial differential operator $\mathscr{L}$, $\mathscr{L}u$ can be approximated by

$$\mathscr{L}u(x) \simeq \sum_{j=1}^{N_c} \lambda_j \mathscr{L}\phi(\|x-\xi_j\|_2) + \mathscr{L}\psi(x). \tag{8}$$

3 The numerical method

3.1 Time discretization

Consider the Ginzburg-Landau equation

$$u_t - (\nu + i\alpha)(u_{xx} + u_{yy}) + (\kappa + i\beta)|u|^2 u - \gamma u = 0, \quad (x,y) \in \Omega,\ t > 0, \tag{9}$$

with periodical boundary conditions (2)-(3) and initial condition (4). For the numerical method, first we discretize the equation (9) according to the following θ-weighted scheme:

$$\frac{u^{n+1}-u^n}{dt} - (\nu + i\alpha)\left[\theta\left(u_{xx}^{n+1} + u_{yy}^{n+1}\right) + (1-\theta)\left(u_{xx}^n + u_{yy}^n\right)\right] + (\kappa + i\beta)\left|u^n\right|^2 u^n - \gamma\left(\theta u^{n+1} + (1-\theta)u^n\right) = 0, \tag{10}$$

where $0 \le \theta \le 1$, dt is the time step size, $u^n = u(x,y,t^n)$ denotes the solution at time $t^n = ndt$. Rearranging (10), using the linear operator $\Delta = (\partial^2/\partial x^2 + \partial^2/\partial y^2)$, we obtain

$$u^{n+1} - \theta dt\left[(\nu + i\alpha)\Delta u^{n+1} + \gamma u^{n+1}\right] = u^n + (1-\theta)dt\left[(\nu + i\alpha)\Delta u^n + \gamma u^n\right] - dt(\kappa + i\beta)\left|u^n\right|^2 u^n. \tag{11}$$

Now we want to apply the radial basis functions for equation (11). Before this, we express that how can use the RBFs to the numerical solution of PDEs.

3.2 Applying the Radial Basis Functions

Assume that there are a total of (N_c-3) interpolation points (centers), the radial basis function expansion of $u^n(x,y)$ can be written as

$$u^n(x,y) \simeq \sum_{j=1}^{N_c-3} \lambda_j^n \phi(r_j) + \lambda_{N_c-2}^n x + \lambda_{N_c-1}^n y + \lambda_{N_c}^n, \quad (x,y) \in \Omega. \tag{12}$$

To determine the coefficients $\lambda_j^n, j = 1,2,\ldots,N_c$, the collocation method is used by applying (12) at every data points $(x_i,y_i), i = 1,2,\ldots,N_d$. Therefore we have

$$u^n(x_i,y_i) \simeq \sum_{j=1}^{N_c-3} \lambda_j^n \phi(r_{ij}) + \lambda_{N_c-2}^n x_i + \lambda_{N_c-1}^n y_i + \lambda_{N_c}^n, \quad i = 1,2,\ldots,N_d, \tag{13}$$

where $r_{ij} = \sqrt{(x_i-x_j)^2+(y_i-y_j)^2}$. The additional solvability conditions of the system for conditionally positive definite RBFs due to (7) are written as

$$\sum_{j=1}^{N_c-3} \lambda_j^n = \sum_{j=1}^{N_c-3} \lambda_j^n x_j = \sum_{j=1}^{N_c-3} \lambda_j^n y_j = 0. \tag{14}$$

The matrix form of the linear system arises from (13) together with (14) is

$$[u]^n = A[\lambda]^n, \tag{15}$$

where

$$A = \begin{bmatrix} \Phi & H \\ T & 0 \end{bmatrix}_{(N_d+3)\times N_c}, \quad \Phi = \left[\phi(r_{ij})\right]_{N_d\times(N_c-3)}, \tag{16}$$

and sub-matrices H and T are obtained from the additional polynomial in (13) and additional conditions (14), respectively.

Since all applied RBFs $\phi(r)$ have global support, so the produced matrices are dense. The coefficients matrix A can be shown to be positive definite (and therefore nonsingular) for distinct centers for Gaussian, inverse multiquadrics and inverse quadric (Dehghan and Shokri, 2007). Also Micchelli (Micchelli, 1986) showed that A is invertible for distinct sets of the scattered points in the case of multiquadrics.

Assume that there are $p < N_d$ internal (domain) points and (N_d-p) boundary points, then the matrix A can be split into: $A = A_d + A_b + A_e$ (for more explanation see (Dehghan and Tatari, 2006)). Using the notation $\mathscr{L}A$ ($\mathscr{L}$ is a linear differential operator) to designate the matrix of the same dimension as A and containing the

elements $\tilde{a}_{ij} = \mathscr{L} a_{ij}$, then from equation (11) together with boundary conditions (2)-(3) and additional conditions (14) we have

$$M_L[\lambda]^{n+1} = M_R[\lambda]^n - [G]^n, \tag{17}$$

where

$$\begin{aligned} M_L &= (1-\theta\gamma dt)A_d - \theta dt(\nu + i\alpha)\Delta A_d + LA_b + A_e, \\ M_R &= (1+(1-\theta)\gamma dt)A_d + (1-\theta)dt(\nu + i\alpha)\Delta A_d, \\ [G]^n &= dt(\kappa + i\beta)\left|U^n\right|^2 U^n \quad , \quad U^n = A_d[\lambda]^n, \end{aligned} \tag{18}$$

and LA_b and A_e are resulting matrices from imposing boundary conditions and additional conditions, respectively.

Since the solution of Ginzburg-Landau equation is complex, so assume that $[\lambda]^n = [\lambda_r]^n + i[\lambda_i]^n$, where r and i indexes mean that real part and imaginary part of complex vector, respectively. Using this notation (17) can be written as

$$\begin{aligned} B[\lambda_r]^{n+1} + D[\lambda_i]^{n+1} + i\left(B[\lambda_i]^{n+1} - D[\lambda_r]^{n+1}\right) = \\ C[\lambda_r]^n - E[\lambda_i]^n - [G_r]^n + i\left(C[\lambda_i]^n + E[\lambda_r]^n - [G_i]^n\right), \end{aligned} \tag{19}$$

where

$$\begin{aligned} B &= (1-\theta\gamma dt)A_d - \theta dt\nu\Delta A_d \quad , \quad D = \theta dt\alpha\Delta A_d, \\ C &= (1+(1-\theta)\gamma dt)A_d + (1-\theta)dt\nu\Delta A_d \quad , \quad E = (1-\theta)dt\alpha\Delta A_d. \end{aligned} \tag{20}$$

The complex equation (19) can be rewritten in the following real variable matrix form:

$$\begin{bmatrix} B & D \\ -D & B \end{bmatrix} \begin{bmatrix} \lambda_r \\ \lambda_i \end{bmatrix}^{n+1} = \begin{bmatrix} C & -E \\ E & C \end{bmatrix} \begin{bmatrix} \lambda_r \\ \lambda_i \end{bmatrix}^{n} - \begin{bmatrix} G_r \\ G_i \end{bmatrix}^{n}. \tag{21}$$

Note that (21) is obtained by equalizing the real and imaginary parts of right and left sides. Thus, the solution of the complex system has been reduced to solving the real variable system.

We performed our computations using Matlab R2010a software. Since the coefficient matrix in (21) is unchanged in time steps and non-square (number of data and interpolation points may be not equal), so we use Moore-Penrose pseudo-inverse routine in Matlab (i.e. pinv) to calculate pseudo-inverse of A only once and use that to find the solutions in each time step of our algorithm.

3.3 The predictor-corrector scheme

To avoid solving the nonlinear system in our method, we moved the non-linear term of the Ginzburg-Landau equation (i.e. $(\kappa+i\beta)|u|^2u$) to the right-hand side and then we carried out the RBF based method. To improve the accuracy of the numerical results, the following predictor-corrector scheme is proposed.

After the first time level (i.e. $[\lambda]^0$, $[\lambda]^1$ are determined by using the initial condition and the previous section's method), for dealing with the non-linearity at time step $(n+1)$, we propose the following (iterative) algorithm

- *Step 1*: Set $U^n = A[\lambda]^n$ and calculate an 'intermediate' value $[\lambda]^{n+1}_{(0)}$ (predictor) from (17) as follows:

$$[\lambda]^{n+1}_{(0)} = M_L^{-1}\left(M_R[\lambda]^n - dt(\kappa+i\beta)\,|U^n|^2U^n\right). \tag{22}$$

  Now set $U^{n+1}_{(0)} = A[\lambda]^{n+1}_{(0)}$ and $U_{(0)} = (U^{n+1}_{(0)} + U^n)/2$. By using these values we get the approximation

$$[\lambda]^{n+1}_{(1)} = M_L^{-1}\left(M_R[\lambda]^n - dt(\kappa+i\beta)\,\left|U_{(0)}\right|^2U_{(0)}\right). \tag{23}$$

- *Step 2*: The general iteration is given by

$$[\lambda]^{n+1}_{(k+1)} = M_L^{-1}\left(M_R[\lambda]^n - dt(\kappa+i\beta)\,\left|U_{(k)}\right|^2U_{(k)}\right), \tag{24}$$

  where $U_{(k)} = (U^{n+1}_{(k)} + U^n)/2$, $U^{n+1}_{(k)} = A[\lambda]^{n+1}_{(k)}$.

- *Step 3*: We iterate the (24) until

$$\frac{\left\|U^{n+1}_{(k+1)} - U^{n+1}_{(k)}\right\|_\infty}{\left\|U^{n+1}_{(k)}\right\|_\infty} \le \varepsilon \text{ for prescribed tolerance } \varepsilon. \tag{25}$$

  or the maximum number of iterations $N \le 50$.

Once the prescribed convergence is achieved, we can move on to the following time level. This process is iterated, until reaching to the desirable time t.

3.4 The boundary treatment

A common feature in all RBF approximations is how relatively inaccurate they are at boundaries (Fornberg, Driscoll, Wright, and Charles, 2002). When approximating wave-type PDEs, large boundary-induced errors of this type can contaminate

the solution everywhere across the domain. Thus, it is necessary to understand how RBFs behave near boundaries and whether there is a way to improve accuracy there. In (Fornberg, Driscoll, Wright, and Charles, 2002) authors suggested some remedies for this problem such as adding polynomial terms to the RBF distribution, Not-a-Knot method, super Not-a-Knot method and clustering of nodes in the boundary.

In our numerical method, to tackle this problem, we choose centers different from data points and add some centers out of the boundary. The centers in contrast with data points in 2D are illustrated in Figure 1. The approximation in the interior is

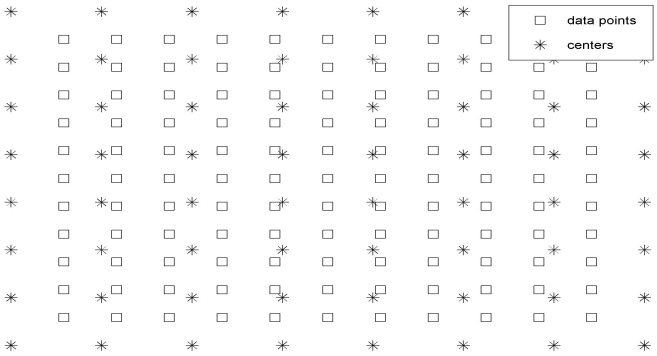

Figure 1: Data points vs. interpolation points (centers).

independent of how far the centers are moved outside of the boundary.

4 Numerical results

In this section, we present some numerical results of our scheme for the Ginzburg-Landau equation. Accuracy of the estimated solutions can be worked out by measuring the L_2 and L_∞ error norms which are defined by

$$L_2 = \left\| u^{exact} - u^{numerical} \right\|_2 = \left(\sum_{i=1}^{N} \left| u_i^{exact} - u_i^{numerical} \right| \right)^{1/2},$$

$$L_\infty = \left\| u^{exact} - u^{numerical} \right\|_\infty = \max_i \left| u_i^{exact} - u_i^{numerical} \right|.$$

Example 1. The plane wave solution

The Ginzburg-Landau equation (1) has the following plane wave solution (Xu and Chang, 2011)

$$u(x,y,t) = ae^{i[\xi(x+y)-\omega t]}, \tag{26}$$

where $a,\ \xi,\ \omega$ are real constants. By substituting (26) in to (1), we will have the following equalities:

$$\begin{cases} \nu\xi^2 + \kappa a^2 - \gamma = 0 \\ -\omega + 2\alpha\xi^2 + \beta a^2 = 0 \end{cases}, \tag{27}$$

from which we have

$$\xi = \pm\sqrt{\frac{\gamma - \kappa a^2}{2\nu}}, \quad \omega = 2\alpha\xi^2 + \beta a^2. \tag{28}$$

Now, we consider the Ginzburg-Landau equation (1) on $\Omega = [0,6] \times [0,6]$ and we take $a = 1.0,\ \nu = 1.0,\ \xi = \frac{\pi}{3},\ T = 2.0$ and $\gamma = \nu\xi^2 + \kappa a^2,\ \omega = 2\alpha\xi^2 + \beta a^2$ from (27). First, we take $\beta = 2.0$ and $\alpha = 0.2,\ 0.4,\ 0.6,\ 0.8,\ 1.0$. The results are tabulated in Table 2 for the thin plate splines (TPS) and the multiquadrics (MQ) with $N_d = N_c = 31,\ \theta = 0.5$ and $dt = 0.01$. The results of our method in comparison with the methods given in (Wang and Guo, 2010) are more accurate. For example, the L_∞ error of scheme 4 (best scheme in (Wang and Guo, 2010)) for $\alpha = 0.2,\ h = 0.2$ is $4.2166(-2)$, but this error for our method is $1.6359(-4)$ for TPS and $2.3073(-3)$ for MQ.

Now, we take $\alpha = 0.2$ and $\beta = -2,\ -1,\ 0,\ 1,\ 2$. The results for TPS and MQ with $N_d = N_c = 31,\ \theta = 0.5$ and $dt = 0.01$ are given in Table 3. As we know from equation (26), $|U|$ is constant. In Figure 2, we plot the $|U|$ for $\alpha = \pm 1$ with $N_d = N_c = 31,\ dt = 0.01$, and $\beta = 2$ at $T = 2$. These figures show that the difference of numerical results from constant is lower than 1 percent.

In Figure 3 we plot the L_2 and L_∞ errors of numerical solution for $N_d = 31$ vs. centers' number at $T = 2$. This figure indicates that when number of centers increases then the error of solution decreases. The best choice for centers number is near the data number.

Table 2. L_2, L_∞ and maximum absolute errors of the method for Example 1 at $T = 2$.

	Maximum absolute error			
	Real part	Imaginary part	L_2	L_∞
$\alpha = 0.2$	7.9725(−3)	1.2435(−2)	2.3986(−1)	1.6359(−4)
	4.5367(−2)	3.0379(−2)	6.5392(−1)	2.3073(−3)
$\alpha = 0.4$	1.5446(−2)	1.4848(−2)	3.1239(−1)	3.3488(−4)
	4.3722(−2)	3.3483(−2)	7.0306(−1)	2.4932(−3)
$\alpha = 0.6$	8.6173(−3)	1.1717(−2)	2.2796(−1)	1.4165(−4)
	3.8083(−2)	3.6015(−2)	7.5281(−1)	2.2437(−3)
$\alpha = 0.8$	1.1588(−2)	1.1014(−2)	2.6954(−1)	1.7748(−4)
	3.3697(−2)	3.6404(−2)	7.9276(−1)	1.8215(−3)
$\alpha = 1.0$	8.3671(−3)	7.8929(−3)	1.6569(−1)	7.0951(−5)
	3.3236(−2)	3.2914(−2)	8.1201(−1)	1.4789(−3)

For every value of α, the first and second rows of data correspond to the using of TPS ($m = 3$) and MQ ($c = 2$) as radial basis function in the method, respectively.

Table 3. L_2, L_∞ and maximum absolute errors of the method for Example 1 at $T = 2$.

	Maximum absolute error			
	Real part	Imaginary part	L_2	L_∞
$\beta = -2$	9.8533(−3)	1.1954(−2)	2.3592(−1)	1.4899(−4)
	3.6143(−2)	3.2630(−2)	5.8452(−1)	1.5756(−3)
$\beta = -1$	6.9036(−3)	6.5710(−3)	1.4180(−1)	4.8942(−5)
	3.3905(−2)	1.4138(−2)	4.7362(−1)	1.1779(−3)
$\beta = 0$	5.7760(−3)	5.1283(−3)	1.4211(−1)	4.0050(−5)
	2.9742(−2)	9.0504(−3)	4.6109(−1)	9.2918(−4)
$\beta = 1$	6.7859(−3)	7.6311(−3)	1.6755(−1)	7.0883(−5)
	3.3819(−2)	1.6740(−2)	5.2367(−1)	1.2886(−3)
$\beta = 2$	7.9725(−3)	1.2435(−2)	2.3986(−1)	1.6359(−4)
	4.5367(−2)	3.0379(−2)	6.5392(−1)	2.3073(−3)

For every value of α, the first and second rows of data correspond to the using of TPS ($m = 3$) and MQ ($c = 2$) as radial basis function in the method, respectively.

In the following two examples, we choose the initial condition in the following form same as (Xu and Chang, 2011)

$$u(x,y,t=0) = u_0(x,y) = A_0(x,y)e^{iS_0(x,y)},\ (x,y) \in \Omega, \tag{29}$$

where $A_0(x,y)$ and $S_0(x,y)$ are known real functions.

Example 2. Zero initial phase data

$$A_0(x,y) = e^{-2x^2-2y^2}, \quad S_0(x,y) = 0. \tag{30}$$

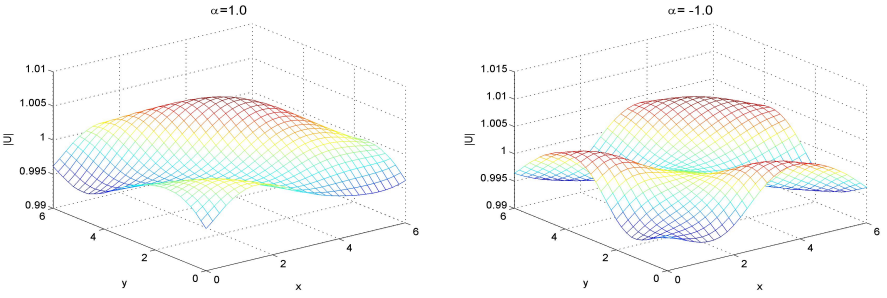

Figure 2: Plot of $|U|$ for Example 1. $\beta = 2.0,\ dt = 0.01,\ N_d = N_c = 31$ and $T = 2$.

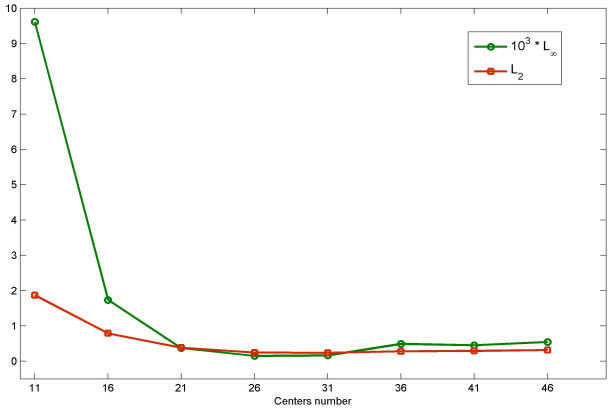

Figure 3: L_2 and L_∞ error of numerical solution for $N_d = 31$ vs. centers' number. $\alpha = 0.2,\ \beta = 2.0,\ dt = 0.01$ and $T = 2$.

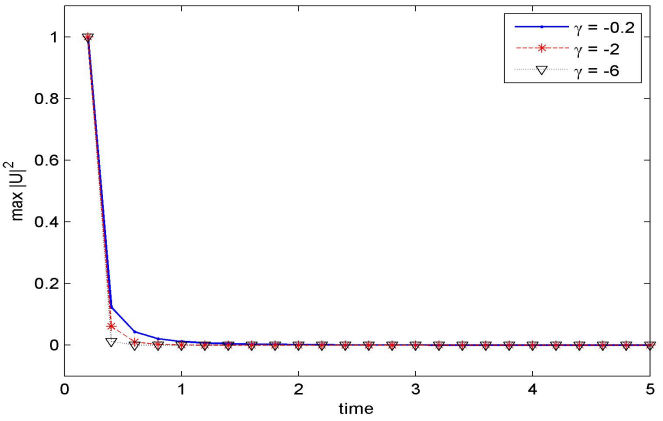

Figure 4: Max $|U|^2$ for Example 2. $\gamma = -0.2,\ -2,\ -6$.

We take the parameters as $\nu = 1.0,\ \alpha = 0.2,\ \kappa = 1.0,\ \beta = 1.0,\ dt = 0.01,\ N_d = N_c = 31$ and we use TPS radial basis function in our computations. With this initial data when $\gamma < 0$ the $||U||_\infty$ decays to zero. As we can see in Figure 4, this decrease is faster when γ is smaller. In Figure 5, the position density $|U|^2$ at $T = 5,\ 10$ with $\gamma = -0.2$ is plotted.

Example 3. Symmetric initial data with nonzero phase

$$A_0(x,y) = e^{-2x^2-2y^2}, \quad S_0(x,y) = \frac{1}{e^{x+y} + e^{-x-y}}. \tag{31}$$

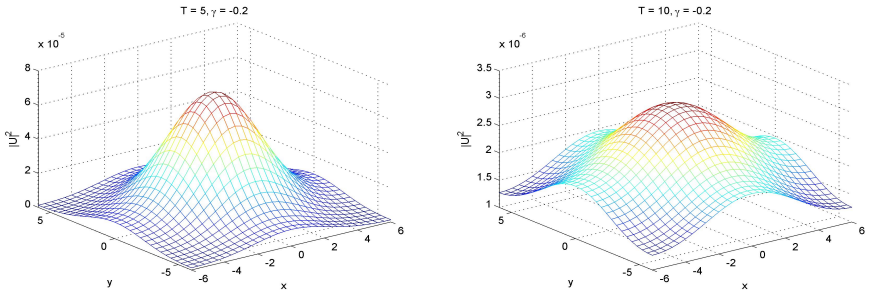

Figure 5: Plot of the position density $|U|^2$ for example 2. $\alpha = 0.2,\ \beta = 1.0,\ dt = 0.01,\ N_d = N_c = 31$.

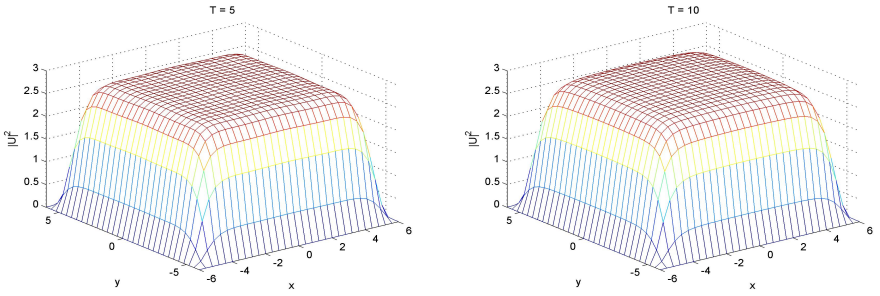

Figure 6: Plot of the position density $|U|^2$ for Example 3. $\alpha = 0.5$, $\beta = 1.0$, $\gamma = 3$, $dt = 0.01$, $N_d = N_c = 31$.

In this example we choose the parameters as $\nu = 1.0$, $\alpha = 0.5$, $\kappa = 1.0$, $\beta = 1.0$, $\gamma = 3$, $dt = 0.01$, $N_d = N_c = 31$ and use TPS as radial basis function. Also, we set the boundary conditions as zero. The plots of results for $T = 5$, 10 are given in Figure 6. To see the influence of parameter β in the solution, we choose the parameter β as -5, -2, 1, 5 and plot the results in Figure 7. The figures are good comparable with the results of (Xu and Chang, 2011).

Example 4. Variable coefficient problem

Consider the following variable coefficient problem

$$u_t - \frac{i}{2}(u_{xx} + u_{yy}) + i|u|^2 u + i(1 - \sin^2(x)\sin^2(y))u = 0, \tag{32}$$

where $(x,y) \in (0,2\pi) \times (0,2\pi)$ and $0 < t \leq T$. The exact solution of this problem is (Wang, 2010)

$$u(x,y,t) = \sin(x)\sin(y)e^{-2ti}. \tag{33}$$

The difference between this problem and Ginzburg-Landau equation is that the coefficient γ in Ginzburg-Landau equation is constant but in this problem it is a function of x and y. The L_2 and L_∞ errors of the numerical solution and CPU time are given in Table 4 for thin plate splines (TPS) with $N_d = 31$, $N_c = 21$, $\theta = 0.5$ and $dt = 0.01$. The obtained results in this table confirm the good accuracy of our method. Also, we plot the density of the solution $|U|$ and the L_∞ error of the solution for $0 < t < 10$ in Figure 8.

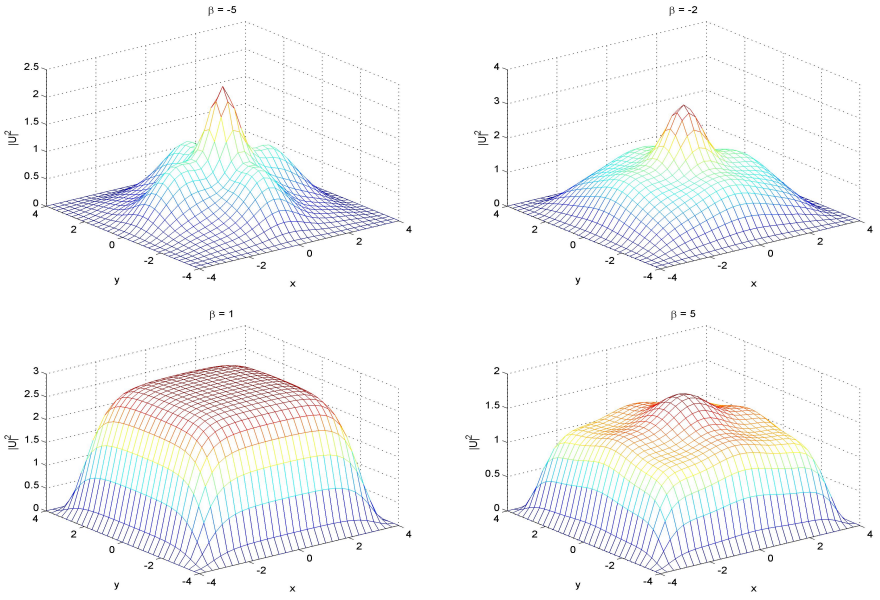

Figure 7: Plot of the position density $|U|^2$ for Example 3. $\alpha = 0.5$, $\gamma = 3$, $dt = 0.01$, $N_d = N_c = 31$ and $T = 5$.

Table 4. L_2, L_∞ and maximum absolute error of the method for Example 4.

	Maximum absolute error				
	Real part	Imaginary part	L_2	L_∞	CPU time
$T = 1$	8.9866(−5)	6.0484(−5)	1.7148(−3)	1.1514(−8)	7.3
$T = 2$	1.9430(−4)	1.3741(−4)	3.3789(−3)	5.6099(−8)	8.3
$T = 3$	9.0752(−5)	3.2916(−4)	4.9671(−3)	1.1658(−7)	9.2
$T = 5$	3.1717(−4)	4.3883(−4)	8.0458(−3)	2.9200(−7)	11.1
$T = 10$	9.5434(−4)	4.6216(−4)	1.5000(−2)	1.1165(−6)	16.0

5 The complex Ginzburg-Landau equation

In this section we will give a brief discussion about impression of the Ginzburg-Landau equation and one of the most important applications of this equation.

The Ginzburg-Landau equation is obtained by minimization of the Ginzburg-Landau free energy functional $F\{\psi, \overrightarrow{A}\}$ with respect to ψ and $\overrightarrow{A}$

$$F\{\psi, \overrightarrow{A}\} = \frac{H_c^2}{4\pi} \int \left[-|\psi|^2 + \frac{1}{2}|\psi|^4 + \frac{1}{2}|(-i\nabla - \overrightarrow{A})\psi|^2 + \kappa^2(\overrightarrow{h} - \overrightarrow{H}_0)^2 \right] dV, \quad (34)$$

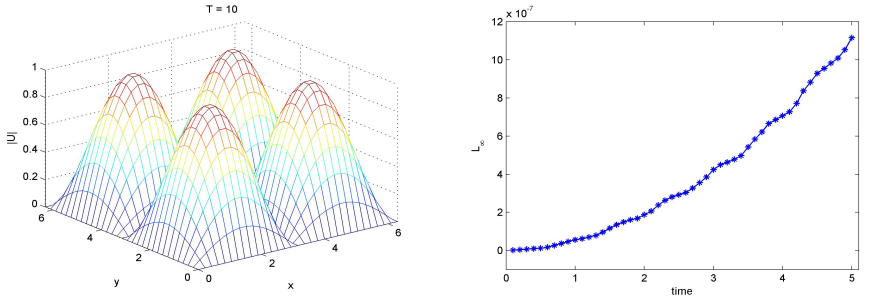

Figure 8: (Left) The position density $|U|$, (Right) L_∞ error of the solution for $0 < t < 10$ for Example 4.

where κ is the Ginzburg-Landau parameter given as a ratio of magnetic penetration depth λ and the coherence length ξ, and H_0 denotes the applied magnetic field(for more information about parameters see (Milošević and Geurts, 2010)).

Every part of Equation (34) describes some physical property. The first part of equation (34) is the expansion of the energy difference between the superconducting and the normal state for a homogeneous superconductor in the absence of an applied magnetic field near the zero-field critical temperature T_{c0}. While, the last term in Equation (34) describes the energy of the magnetic field of the supercurrents, which measures the response of the superconductor to an external field and is nothing else than the difference between the local and applied magnetic fields (Milošević and Geurts, 2010).

The phenomenological Ginzburg-Landau theory is one of the most elegant and powerful concepts in physics. Grossauer and Scherzer (Grossauer and Scherzer, 2003) proposed the Ginzburg-Landau equation for digital inpainting purposes.

Solutions of the real valued Ginzburg-Landau equation develop areas with values ± 1, which are separated by phase transition regions. This property makes the real valued Ginzburg-Landau equation a reasonable method for high quality inpainting of binary images, i.e., level sets (Borzi, Grossauer, and Scherzer, 2005). In (Borzi, Grossauer, and Scherzer, 2005; Grossauer and Scherzer, 2003) the authors used the complex valued Ginzburg-Landau equation for inpainting of gray-valued and color images.

As is said in (Borzi, Grossauer, and Scherzer, 2005), the solution of the Ginzburg-Landau equation reveals high contrast in the inpainting domain, which makes it particularly suited for inpainting purposes. However, the level lines of the solution of the Ginzburg-Landau equation at the boundary of the inpainting domain might

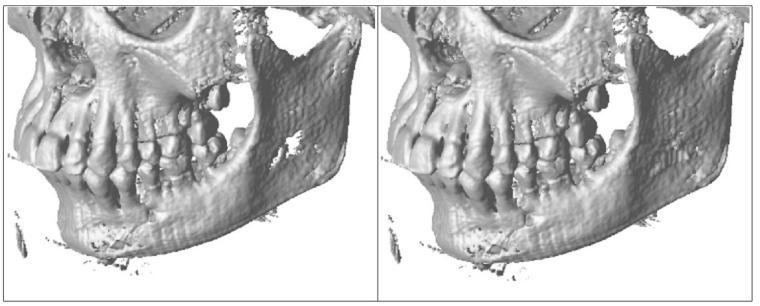

Figure 9: The hole in the cheekbone has been filled.

look kinky.

The Ginzburg-Landau equation can be generalized to any number of space dimension. Thus in particular it can be applied to inpaint three dimensional grey valued image intensity functions (Grossauer and Scherzer, 2003). A more realistic application is shown in Figure 9 where Grossauer and Scherzer (Grossauer and Scherzer, 2003) used their inpainting algorithm based on the solutions of the Ginzburg-Landau equation to fill a hole in the left cheekbone. As is mentioned in (Grossauer and Scherzer, 2003), using this kind of processing for medical data is quite dangerous but could be useful for refinement of data obtained in heritage recording projects.

6 Conclusion

In this article we presented a numerical simulation of the nonlinear 2D complex Ginzburg-Landau equation using collocation and approximating the solution by MQ and TPS radial basis functions (RBFs). To improve the accuracy on the boundary we chose centers different from data points and added some centers out of the boundary. Also, to avoid solving nonlinear system, the predictor-corrector scheme is used. In the simulation of the plane wave solution and variable coefficient problem, high accuracy has been achieved by comparing the numerical solutions with the exact ones in terms of the L_2 and L_∞ error norms. In the zero initial phase data and symmetric initial data with nonzero phase cases results are good comparable with the results of other researchers. The numerical results given in the previous section demonstrate the efficiency and good accuracy of the new method.

Acknowledgement: The authors are very grateful to the reviewers for their com-

ments.

References

Adibi, H.; Es'haghi, J. (2007): Numerical solution for biharmonic equation using multilevel radial basis functions and domain decomposition methods. *Applied Mathematics and Computation*, vol. 186, pp. 246–255.

Askerzade, I. N. (2010): Numerical Simulation of Vortex Nucleation in the Two-Band Ginzburg-Landau Model. *Technical Physics*, vol. 55, no. 6, pp. 896–899.

Atluri, S. N. (2005): *The meshless method (MLPG) for domain and BIE discretizations*. Tech Science Press, Encino, CA.

Atluri, S. N.; Shen, S. (2002): *The Meshless Local Petrov-Galerkin (MLPG) Method*. Tech Science Press, Encino, CA.

Atluri, S. N.; Shen, S. (2002): The meshless local Petrov-Galerkin (MLPG) method: a simple and lesscostly alternative to the finite element and boundary element methods. *CMES: Computer Modeling in Engineering and Sciences*, vol. 3, pp. 11–52.

Atluri, S. N.; Shen, S. (2005): The basis of meshless domain discretization: the meshless local Petrov-Galerkin (MLPG) method. *Adv. Comput. Math.*, vol. 23, pp. 73–93.

Atluri, S. N.; Zhu, T. (1998): A new meshless local Petrov-Galerkin (MLPG) approach in computational mechanics. *Computational Mechanics*, vol. 22, pp. 117–127.

Borzi, A.; Grossauer, H.; Scherzer, O. (2005): Analysis of iterative methods for solving a Ginzburg-Landau equation. *International Journal of Computer Vision*, vol. 64, no. 2/3, pp. 203–219.

Brown, D.; Ling, L.; Kansa, E.; Levesley, J. (2005): On approximate cardinal preconditioning methods for solving PDEs with radial basis functions. *Engineering Analysis with Boundary Elements*, vol. 29, pp. 343–353.

Carlson, R. E.; Foley, T. A. (1991): The parameter r^2 in multiquadric interpolation. *Computers and Mathematics with Applications*, vol. 21, no. 9, pp. 29–42.

Chang, W.; Ankiewicz, A.; Akhmediev, N. (2007): Creeping solitons of the complex Ginzburg-Landau equation with a low-dimensional dynamical system model. *Physics Letters A*, vol. 362, pp. 31–36.

Chen, Z. (1997): Mixed finite element methods for a dynamical Ginzburg-Landau model in super-conductivity. *Numerical Mathematics*, vol. 76, pp. 323–353.

Cheng, A. H. D.; Golberg, M. A.; Kansa, E. J.; Zammito, T. (2003): Exponential convergence and h-c multiquadric collocation method for partial differential equations. *Numerical Methods for Partial Differential Equations*, vol. 19, no. 5, pp. 571–594.

Dehghan, M.; Ghesmati, A. (2010): Combination of meshless local weak and strong (MLWS) forms to solve the two dimensional hyperbolic telegraph equation. *Engineering Analysis with Boundary Elements*, vol. 34, pp. 324–336.

Dehghan, M.; Mirzaei, D. (2009): Meshless local Petrov-Galerkin (MLPG) method for the unsteady magnetohydrodynamic (MHD) flow through pipe with arbitrary wall conductivity. *Applied Numerical Mathematics*, vol. 59, pp. 1043–1058.

Dehghan, M.; Salehi, R. (2011): A boundary-only meshless method for numerical solution of the Eikonal equation. *Computational Mechanics*, vol. 47, pp. 283–294.

Dehghan, M.; Shokri, A. (2007): A numerical method for two-dimensional Schrödinger equation using collocation and radial basis functions. *Computers and Mathematics with Applications*, vol. 54, pp. 136–146.

Dehghan, M.; Shokri, A. (2009): A meshless method for numerical solution of the one-dimensional wave equation with an integral condition using radial basis functions. *Numerical Algorithms*, vol. 52, pp. 461–477.

Dehghan, M.; Tatari, M. (2006): Determination of a control parameter in a one-dimensional parabolic equation using the method of radial basis functions. *Mathematical and Computer Modelling*, vol. 44, pp. 1160–1168.

Demirkaya, G.; Soh, C. W.; Ilegbusi, O. J. (2008): Direct solution of Navier-Stokes equations by radial basis functions. *Applied Mathematical Modelling*, vol. 32, pp. 1848–1858.

Divo, E.; Kassab, A. J. (2005): A meshless method for conjugate heat transfer problems. *Engineering Analysis with Boundary Elements*, vol. 29, pp. 136–149.

Duan, Y.; Tan, Y. (2006): On condition number of meshless collocation method using radial basis functions. *Applied Mathematics and Computation*, vol. 172, no. 1, pp. 141–147.

Duan, Y.; Tang, P. F.; Huang, T. Z.; Lai, S. J. (2009): Coupling projection domain decomposition method and Kansa's method in electrostatic problems. *Computer Physics Communications*, vol. 180, pp. 209–214.

Fasshauer, G. E. (1996): *In: Le Méchauté A, Rabut C, Schumaker LL, editors. Solving partial differential equations by collocation with radial basis functions*. proceedings of Chamonix, vol. 1-8. Nashville, TN: Vanderbilt University Press.

Fedoseyev, A. I.; Friedman, M. J.; Kansa, E. J. (2000): Continuation for nonlinear elliptic partial differential equations discretized by the multiquadric method. *International Journal of Bifurcation and Chaos*, vol. 10, no. 2, pp. 481–492.

Fedoseyev, A. I.; Friedman, M. J.; Kansa, E. J. (2002): Improved multiquadric method for elliptic partial differential equations via PDE collocation on the boundary. *Computers and Mathematics with Applications*, vol. 43, no. 3-5, pp. 439–455.

Fornberg, B.; Driscoll, T. A.; Wright, G.; Charles, R. (2002): Observations on the behavior of radial basis function approximations near boundaries. *Computers and Mathematics with Applications*, vol. 43, pp. 473–490.

Ginzburg, V. L.; Landau, L. D. (1950): To the theory of superconductivity. *Journal of Experimental and Theoretical Physics*, vol. 20, pp. 1064–1082.

Golberg, M. A.; Chen, C. S.; Ganesh, M. (2000): Particular solutions of 3D Helmholtz-type equations using compactly supported radial basis functions. *Engineering Analysis with Boundary Elements*, vol. 24, pp. 539–547.

Grossauer, H.; Scherzer, O. (2003): *Using the complex Ginzburg-Landau equation for digital inpainting in 2D and 3D, Scale Space Methods in Computer Vision, Lecture Notes in Computer Science 2695*. Springer.

H. Fu, Z. D. (2010): Exact chirped solitary-wave solutions for Ginzburg-Landau equation. *Communications in Nonlinear Science and Numerical Simulation*, vol. 15, pp. 1462–1465.

Hardy, R. L. (1990): Theory and applications of the multiquadric-biharmonic method. 20 years of discovery 1968-1988. *Computers and Mathematics with Applications*, vol. 10, no. 8/9, pp. 163–208.

Hon, Y. C.; Schaback, R. (2001): On unsymmetric collocation by radial basis functions. *Applied Mathematics and Computation*, vol. 119, pp. 177–186.

Kansa, E. J. (1990): Multiquadrics - A scattered data approximation scheme with applications to computational fluid dynamics - I. *Computers and Mathematics with Applications*, vol. 19, pp. 127–145.

Kansa, E. J. (1990): Multiquadrics - A scattered data approximation scheme with applications to computational fluid dynamics - II. *Computers and Mathematics with Applications*, vol. 19, pp. 147–161.

Kolesov, A. Y.; Rosov, N. K. (2000): Characteristic features of the dynamics of the Gingzburg-Landau equation in a plane domain. *Theoretical and Mathematical Physics*, vol. 125, no. 2, pp. 1476–1488.

Lega, J. (2001): Traveling hole solutions of the complex Ginzburg-Landau equation: a review. *Physica D*, vol. 152-153, pp. 269–287.

Liu, J.; Li, Y.; Tian, B. (2009): Soliton-like solutions for the modified variable-coeficient Ginzburg-Landau equation. *Communications in Nonlinear Science and Numerical Simulation*, vol. 14, pp. 1214–1226.

Micchelli, C. A. (1986): Interpolation of scattered data: Distance matrices and conditionally positive definite functions. *Constructive Approximation*, vol. 2, pp. 11–22.

Milošević, M. V.; Geurts, R. (2010): The Ginzburg-Landau theory in application. *Physica C*, vol. 470, pp. 791–795.

Mirzaei, D.; Dehghan, M. (2010): A meshless based method for solution of integral equations,. *Applied Numerical Mathematics*, vol. 60, pp. 245–262.

Platte, R. B.; Driscoll, T. A. (2004): Computing eigenmodes of elliptic operators using radial basis functions. *Computers and Mathematics with Applications*, vol. 48, pp. 561–576.

Rippa, S. (1999): An algorithm for selecting a good parameter c in radial basis function interpolation. *Advances in Computational Mathematics*, vol. 11, pp. 193–210.

Rocca, A. L.; Rosales, A. H.; Power, H. (2005): Radial basis function Hermite collocation approach for the solution of time dependent convection-diffusion problems. *Engineering Analysis with Boundary Elements*, vol. 29, pp. 359–370.

Sarra, S. A. (2005): Adaptive radial basis function methods for time dependent partial differential equations. *Applied Numerical Mathematics*, vol. 54, pp. 79–94.

Sarra, S. A.; Sturgill, D. (2009): A random variable shape parameter strategy for radial basis function approximation methods. *Engineering Analysis with Boundary Elements*, vol. 33, pp. 1239–1245.

Schaback, R. (1995): Error estimates and condition numbers for radial basis function interpolation. *Advances in Computational Mathematics*, vol. 3, no. 3, pp. 251–264.

Schaback, R. (1995): *Multivariate interpolation and approximation by translates of a basis function, In: Approximation Theory VIII, vol. 1 (College Station, TX, 1995). Ser Approx Decompos. vol. 6*. River Edge, NJ: World Scientific.

Schaback, R. (1997): *On the efficiency of interpolation by radial basis functions, In: Surface fitting and multiresolution methods (Chamonix-Mont-Blanc, 1996)*. Nashville, TN: Vanderbilt University Press 309-318.

Schaback, R.; Franke, C. (1998): Covergence order estimates of meshless collocation methods using radial basis functions. *Advances in Computational Mathematics*, vol. 8, no. 4, pp. 381–399.

Sladek, J.; Sladek, V.; Atluri, S. N. (2004): Meshless local Petrov-Galerkin method for heat conduction problem in an anisotropic medium. *CMES: Computer Modeling in Engineering and Sciences*, vol. 6, pp. 309–318.

Sladek, J.; Sladek, V.; Hellmich, C.; Eberhardsteiner, J. (2007): Heat conduction analysis of 3D axisymmetric and anisotropic FGM bodies by meshless local Petrov-Galerkin method. *Computational Mechanics*, vol. 39, pp. 223–233.

Sladek, J.; Sladek, V.; Krivacek, J.; Zhang, C. (2003): Local BIEM for transient heat conduction analysis in 3-D axisymmetric functionally graded solids. *Computational Mechanics*, vol. 32, pp. 169–176.

Sladek, J.; Sladek, V.; Tan, C.; Atluri, S. N. (2008): Analysis of transient heat conduction in 3D anisotropic functionally graded solids, by the MLPG method. *CMES: Computer Modeling in Engineering and Sciences*, vol. 32, pp. 161–174.

Sladek, J.; Sladek, V.; Zhang, C. (2004): A local BIEM for analysis of transient heat conduction with nonlinear source terms in FGMs. *Engineering Analysis with Boundary Elements*, vol. 28, pp. 1–11.

Tatari, M.; Dehghan, M. (2009): On the solution of the non-local parabolic partial differential equations via radial basis functions. *Appl. Math. Modelling*, vol. 33, pp. 1729–1738.

Wang, B. (1999): Existence of time periodic solutions for the Ginzburg-Landau equations of superconductivity. *Journal of Mathematical Analysis and Applications*, vol. 232, pp. 394–412.

Wang, H. (2010): An efficient Chebyshev-Tau spectral method for Ginzburg-Landau-Schrödinger equations. *Computer Physics Communications*, vol. 181, pp. 325–340.

Wang, T.; Guo, B. (2010): Analysis of some finite difference schemes for two-dimensional Ginzburg-Landau equation. *Numerical Methods for Partial Differential Equations*, vol. 27, no. 5, pp. 1340–1363.

Wazwaz, A. M. (2009): *Partial Differential Equations and Solitary Waves Theory*. Springer, New York.

Wendland, H. (1995): Piecewise polynomial, positive definite and compactly supported radial functions of minimal degree. *Advances in Computational Mathematics*, vol. 4, pp. 389–396.

Wu, Z. (1992): Hermite-Birkhoff interpolation of scatterd data by radial basis functions. *Approximation theory*, vol. 8, no. 2, pp. 1–11.

Wu, Z. (1998): *Solving PDE with radial basis function and the error estimation*. In: Chen Z, Li Y, Micchelli CA, Xu Y, Dekker M, Guang Zhou, editors. Advances

in computational mathematics, lecture notes on pure and applied mathematics, vol. 202.

Xu, Q.; Chang, Q. (2011): Difference methods for computing the Ginzburg-Landau equation in two dimensions. *Numerical Methods for Partial Differential Equations*, vol. 27, no. 3, pp. 507–528.

Zhan, M. Q. (2000): Existence of periodic solutions for Ginzburg-Landau equations of superconductivity. *Journal of Mathematical Analysis and Applications*, vol. 249, pp. 614–625.

Zhan, M. Q. (2008): Multiplicity and stability of time-periodic solutions of Ginzburg-Landau equations of superconductivity. *Journal of Mathematical Analysis and Applications*, vol. 340, no. 1, pp. 126–134.

Zhang, Y. (2007): Solving partial differential equations by meshless methods using radial basis functions. *Applied Mathematics and Computation*, vol. 185, pp. 614–627.

Zhu, T.; Zhang, J.; Atluri, S. N. (1998): A local boundary integral equation (LBIE) method in computational mechanics, and a meshless discretization approach. *Computational Mechanics*, vol. 21, pp. 223–235.